Carbohydrate Polymers 241 (2020) 116274

Contents lists available at ScienceDirect

Carbohydrate Polymers

journal homepage: www.elsevier.com/locate/carbpol

Effects of silylated starch structure on hydrophobization and mechanical properties of thermoplastic starch foams made from potato starch

Bruno Felipe Bergel[a,*], Ludmila Leite Araujo[a], André Luís dos Santos da Silva[b], Ruth Marlene Campomanes Santana[a]

[a] Polymeric Materials Lab, Materials Engineering Department, Federal University of Rio Grande do Sul, Av. Bento Gonçalves, 9500, P.O. Box 15090, ZC 91501-970 Porto Alegre, RS, Brazil
[b] SENAI Institute of Innovation in Polymer Engineering, Av. Presidente João Goulart, 682, ZC 93030-090 São Leopoldo, RS, Brazil

ARTICLE INFO

Keywords:
TPS foam
3-chloropropyl trimethoxysilane
Methyltrimethoxysilane
Silylated starch

ABSTRACT

Non-biodegradable single use packaging are a serious environmental problem as it generates large amounts of waste and is generally not recycled. These packages, especially those made of expanded polystyrene, can be replaced by thermoplastic starch foams. These foams have the advantage of being from renewable sources and biodegradable. However, this material is hydrophilic and becomes unusable when it is exposed to water. Hydrophobizing starch comes as an alternative to make the foams more resistant to contact with water. The purpose of the modification is to exchange starch hydroxyl groups for less polar groups such as silane groups. In this work, two silanes were used for starch silylation: 3-chloropropyl trimethoxysilane and Methyltrimethoxysilane. The foams were made using four materials: modified starch, gelatinized starch, polyvinyl alcohol and water. Results from water absorption tests and mechanical tests show that foams absorb less water and become more resistant with the addition of silylated starch.

1. Introduction

Single use packaging of non-biodegradable plastics has been widely used as packaging of various products, mainly food. As these packages are discarded shortly after consumption, a large amount of waste is produced. Recently several organizations have warned about the impact of these plastics on the environment and some localities have already adopted measures such as banning plastic bags and straws (Clemente, Paresque, & Santos, 2018; Compa et al., 2019; Dikareva & Simon, 2019; Jepsen & de Bruyn, 2019; Menicagli, Balestri, Vallerini, Castelli, & Lardicci, 2019). In this context, thermoplastic starch (TPS) foams have attracted the interest of society, as it can replace disposable packaging made with expanded polystyrene (EPS) (such as plates, boxes and cups). As starch is an abundant, relatively inexpensive and biodegradable natural source polymer, products based on this material have become interesting. TPS foams are affordably produced using only starch, water and plasticizer. A starch paste is then formed and placed in a closed mold and heated for a few minutes. This method easily produces foams of various shapes as the material takes the shape of the mold. Due to the easily production these materials can be useful in many applications (Glenn, Orts, & Nobes, 2001; Soykeabkaew, Thanomsilp, & Suwantong, 2015). Notwithstanding, these foams have limited use due to their lack of moisture resistance and their great brittleness. Starch has three hydroxyl groups on each α-glucose monomer. These hydroxyls tend to form hydrogen bonds with the surrounding moisture, which results in a hydrophilic nature. Due to hydrophilicity, starch materials may collapse and disintegrate in contact with water and in humid environments tend to lose mechanical strength (Bergel, da Luz, & Santana, 2017; Bergel, da Luz, & Santana, 2018; Shogren, Lawton, Doane, & Tiefenbacher, 1998).

One way to overcome or decrease the hydrophilicity of TPS foams is to chemically modify the starch by removing its hydroxyl groups and adding less polar groups such as acetyl or silyl groups (Bergel, Dias Osorio, da Luz, & Santana, 2018; Petzold, Koschella, Klemm, Heublein, & Jena, 2003; Volkert, Lehmann, Greco, & Nejad, 2010). Foams with acetylated starch and esterified starch with maleic anhydride were analyzed in a previous study (Bergel, da Luz et al., 2018).

Silicon compounds are well established in organic and polymeric chemistry. The silylation of polar functional groups (such as −OH, –NHR, –SH, −COOH) leads to a noticeable increase in their lipophilic behavior, as well as a drastic increase in the thermal stability of molecules. In the case of alcohols, silylation usually occurs with the corresponding chlorosilanes or silazanes, resulting in the formation of silyl ethers. Silylated starches have been used as adhesives, binders,

* Corresponding author.
E-mail address: bruno.bergel@ufrgs.br (B.F. Bergel).

https://doi.org/10.1016/j.carbpol.2020.116274
Received 28 December 2019; Received in revised form 7 April 2020; Accepted 7 April 2020
Available online 25 April 2020
0144-8617/

Table 1
Formulation of the analyzed foams.

Sample	Dry starch (g)	CPMS starch (g)	MTMS starch (g)	Gel. starch (g)	PVOH (g)	Water (mL)	Proportion of silylated starch in paste (%)
TPS	47	0	0	47	6	50	0
TPS-CPMS.10	37	10	0	47	6	50	6.67
TPS-CPMS.20	27	20	0	47	6	50	13.34
TPS-CPMS.30	17	30	0	47	6	50	20
TPS-CPMS.40	7	40	0	47	6	50	26.67
TPS-MTMS.10	37	0	10	47	6	50	6.67
TPS-MTMS.20	27	0	20	47	6	50	13.34
TPS-MTMS.30	17	0	30	47	6	50	20
TPS-MTMS.40	7	0	40	47	6	50	26.67

coatings, repellents, flocculating agents and in the composition of glass fibers (Petzold et al., 2003; Qu & He, 2013; Zollfrank, 2001). In recent years, the use of silylated starches as coupling agents between two non-compatible phases has been studied. For example, the compatibility between polyethylene and starch is more successful when the starch is pretreated with sodium alkyl silicate (Jariyasakoolroj & Chirachanchai, 2014; Qi et al., 2006). Wu, Qi, Liang, and Zhang (2006) demonstrated that the interfacial adhesion between rubber and starch improved when the starch was coupled with N- (aminoethyl) aminopropyl trimethoxysilane. Jariyasakoolroj and Chirachanchai (2014) modified starch with a chlorosilane to improve adhesion between starch and PLA. The resulting silylated starches had a degree of substitution (DS) between 0.4 and 0.5 and showed hydrophobic characteristics. PLA/silylated starch blends had some improvements in their mechanical properties, demonstrating a greater compatibility between the two phases. Silylated starches have hydrophobic properties even at low DS, which makes them insoluble in water. At higher DS this starch becomes insoluble in most organic solvents (methanol, ethanol, DMSO, ethyl acetate, tetrahydrofuran, chloroform, dichloromethane and hexane). Starch silylation also increases the viscosity of starch pastes, even at low DS, indicating the formation of complexes or crosslinks (Blackwell, Foster, Beck, & Piers, 1999; Mormann & Wagner, 1997; Petzold et al., 2003; Qu & He, 2013; Staroszczyk & Janas, 2010; Staroszczyk, 2009; Wang, Guan, Seib, & Shi, 2018; Wei et al., 2016).

Thus, the objective of this work was to analyze and compare TPS foams produced with silylated starches obtained with silanes of different chemical structures. The proportion of silylated starch in the foams was also analyzed. For the modifications, two different silanes were tested: 3-chloropropyl trimethoxysilane (CPMS) and methyltrimethoxysilane (MTMS). All foams were produced by the baking/compression method. The incorporation of silane groups in starch was analyzed by Fourier transform infrared spectroscopy (FT-IR) and nuclear magnetic resonance (NMR). The foams were characterized by contact angle, water absorption, flexural strength and impact strength, morphology was analyzed by scanning electron microscopy (SEM).

2. Materials and preparation

2.1. Materials

Potato starch (Giro Verde®) was purchased at Porto Alegre public market in Rio Grande do Sul, Brazil. The average size of the potato starch granules is 57.5 μm and the amylose content is 18 %. 3-chloropropyl trimethoxysilane (CPMS) and Methyltrimethoxysilane (MTMS) were purchased from Sigma-Aldrich® with 98 % purity. Potassium hydroxide and polyvinyl alcohol (PVOH) were purchased from Neon®.

2.2. Starch silylation

To perform the silylation reaction, 19.8 mL of CPMS (0.1 mol) was stirred in 300 mL of deionized water at 50 °C until the turbidity of the solution completely disappeared. Then 32.4 g (0.2 mol) of starch previously dried in an oven and 2 g of potassium hydroxide were added. The mixture was kept under stirring at 50 °C under vacuum for 4 h. The product was then filtered and placed in an oven at 70 °C for 24 h. Then the dried product is purified by washing it twice in tetrahydrofuran before being placed in the oven again for another 24 h (Jariyasakoolroj & Chirachanchai, 2014). The molar feeding ratio between silane and starch was 0.5:1, chosen after a previous study to determine the ideal condition of the reaction. The reaction using MTMS (0.1 mol, 14.2 mL) was made similarly.

2.3. Foam preparation

Four components (PVA, water, dry starch and gelatinized starch) were mixed to obtain the starch pastes. It was decided to gelatinize a portion of the starch to improve the dispersion of the formulation components, retaining the solid components in the paste and thus forming a more homogeneous paste with adequate viscosity (Carr, Parra, Ponce, Lugão, & Buchler, 2006). To produce gelatinized starch, 20 g of starch was added to 100 mL of water at 70 °C. After the gelatinized starch was cooled, dry starch and PVOH plasticizer diluted with distilled water were added. The mixtures were made with the aid of a mechanical stirrer until complete homogenization. The paste produced was placed in a preheated mold at 180 °C and then compressed into a 2.5 t hydraulic press for 240 s. The mold used has the following proportions: 150 mm in length, 150 mm in width and 3 mm in thickness. All analyzed foams adequately filled the mold. Samples with formation problems were discarded. The foams produced were stored at room temperature. Table 1 presents the formulation of the samples produced. Silylated starches replace dry starch in the mixture. The proportion of silylated starch was calculated based on the weight of the paste (with all components added, including water) prior to the foaming process.

2.4. Characterization of the silylated starches

2.4.1. Fourier transform infrared spectroscopy

To evaluate the functional groups of the silylated starches, Fourier transform infrared spectroscopy (Perkin-Elmer frontier equipment) was used. Starch samples were macerated and homogenized with KBr to form pellets used to obtain spectra. The analyses were performed by transmittance in the range of $4000-400\ cm^{-1}$, 30 scans at room temperature (~20 °C), according to ASTM E 1252.

2.4.2. Nuclear magnetic resonance spectroscopy and determination of degree of substitution

To evaluate the results of silylation reactions and the chemical structure of silylated starches, ^{1}H and ^{29}Si nuclear magnetic resonance (RMN) spectroscopy was used. The ^{1}H NMR spectra were made on a Bruker spectrometer, Ascend model with Avance IIIHD console, operating at a frequency of 400 MHz. Deuterated dimethyl sulfoxide (DMSO-d_6) was the NMR solvent. ^{29}Si NMR spectra were obtained on an Agilent spectrometer with DD2 console, operating at a frequency of 99.32 MHz.

The degree of substitution (DS) was determined experimentally using a method based on the methods described by Petzold et al. (2003) and Staroszczyk and Janas (2010). Samples of 200 mg of silylated starch were placed in solution containing 10 mL of sulfuric acid and 10 mL of nitric acid for 48 h. Afterwards, the solution was heated until the acids were fully boiled. The remaining residue was placed in an oven at 100 °C. Then the product was placed in 10 mL hydrochloric acid for 3 h and then placed in the oven again. After weighing the final product, the DS was calculated from the Eq. (1) (Klemm, Philipp, Heinze, Heinze, & Wagenknecht, 2004):

$$DS = \frac{M_{AGU}}{\frac{M_{SiO_2}\, x\, 100\%}{m\%SiO_2} - (M_{AGU} - M_H)} \quad (1)$$

Where M_{AGU} is the molar mass of the starch, M_{SiO2} is the molar mass of SiO_2, m%SiO_2 is the percentage of SiO_2 present in the sample after the reaction of the starch with the acids, M_H is the molar mass of the substituent.

2.5. Characterization of the foams

2.5.1. Density

Foam density was determined by sample weight (Kg) /sample volume (m^3). Weight, thickness, width and length measurements were made in triplicate according to ASTM D1622 − 08 (Shogren, Lawton, Doane et al., 1998).

2.5.2. Scanning electron microscopy

Cross-sectional images of the foam samples were studied using a JEOL JSM 6060 scanning electron microscope (SEM) operating at 5 kV voltage acceleration. The samples were metallized with gold. Average cell size and cell density (number of cells per unit volume) were evaluated using ImageJ software. Cell density was calculated using the Eq. (2):

$$Nf = \left(\frac{nM^2}{A}\right)^{3/2} \cdot \left(\frac{1}{1 - Vf}\right) \quad (2)$$

Where Vf is the void content, Nf is the cell density (cells/cm^3), n is the number of cells in the micrograph, A is the area of the micrograph (cm^2) and M is the magnification of the micrograph.

2.5.3. Contact angle

This test is based on the wettability of the sample surface, which involves observing a sessile drop of the test liquid on a solid substrate. ASTM D7334 was used as base and distilled water as test liquid. Image acquisition was performed using a digital optical microscope and contact angle (θ) calculations were performed automatically by an image analysis software.

2.5.4. Water absorption

Foam samples measuring 4 cm × 2 cm were weighed and placed in contact with water (not dipped) for 5 min. After removing excess water, the samples were reweighed. The amount of water absorbed was calculated gravimetrically, and the analysis was done in triplicate for each formulation according to ABNT, 1999 (Vercelheze et al., 2012).

2.5.5. Moisture content

Previously dried samples measuring 4 cm in length and 3 cm in width were weighed and placed in sealed containers containing 90 % relative humidity. These containers were then placed in an oven at 25 °C. A solution with 20 % w/w sulfuric acid was placed in each container to keep the humidity stable. The absorbed moisture was calculated by the difference in the weight of the samples before and after exposure to the humid environment for 24, 48, 72, 96 and 120 h (Bénézet, Stanojlovic-Davidovic, Bergeret, Ferry, & Crespy, 2012; Glenn et al., 2001). The data obtained were adjusted to a mathematical model proposed by Peleg (1988) to study the absorption kinetics. This model is presented in Eq. (3):

$$M_{(t)} = M_0 + \left(\frac{t}{(K_1 + K_2 t)}\right) \quad (3)$$

Where $M_{(t)}$ is the moisture in time, M_0 is the initial moisture, t is the time, K1 is the Peleg flux constant (h/(w water /w solids)), while K2 is Peleg capacity constant (w solids /w water). Statistic Statsoft for Windows 10 software was used to perform statistical analysis. The test was done in triplicate for each sample.

2.5.6. Mechanical tests

The flexure test was performed on an INSTRON universal test machine, model 3382, according to ASTM D790 at a test speed of 1 mm/min. The sample dimensions were 100 mm x 25 mm x 3 mm. The results obtained are the average test of at least five independent specimens for each formulation.

Impact IZOD strength test was carried out with ASTM D256 on IMPACTOR II. A 0.5 J hammer was used. The samples tested were the following measures: 60 mm x 12 mm x 3 mm. The results obtained were the mean values of 7 samples for each formulation independently analyzed. The analysis took place at room temperature (25 °C) and relative humidity of 40–60 %.

3. Results and discussion

3.1. Characterization of modified starches

The FTIR spectra of the TPS (A) and the two modified starches, TPS-CPMS (B) and TPS-MTMS (C), are shown in Fig. 1. In Fig. 1A spectra it was observed the characteristic peaks of the TPS: a wide peak in the range of 3400 − 3200 cm^{-1} attributed to the elongation of O—H bonds; a peak at 2925 cm^{-1} attributed to elongation of C–H bonds; a peak between 1644 − 1625 cm^{-1} corresponding to angular deformation of O—H bonds, a peak between 1400 − 1300 cm^{-1} corresponding to symmetrical and asymmetric vibrations of C–H bonds. The strong peak between 1200 − 1000 cm^{-1} corresponds to the elongation and vibration of the C—O—C bonds and the elongation and vibration of the C—O bonds linked to hydroxyls (Lima et al., 2012; Wokadala, Emmambux, & Ray, 2014). Although the characteristic peaks of the Si-O − CH_2 group (between 1150 − 1000 cm^{-1}), which prove the coupling of silanes with starch, are in the same range as the C—O—C group, some characteristic peaks of CPMS and MTMS can be noted. In Fig. 1B a small peak between 1275 − 1320 cm^{-1} and a strong peak between 890 − 860 cm^{-1} can be observed, these peaks correspond to the elongation of C-Cl bonds and

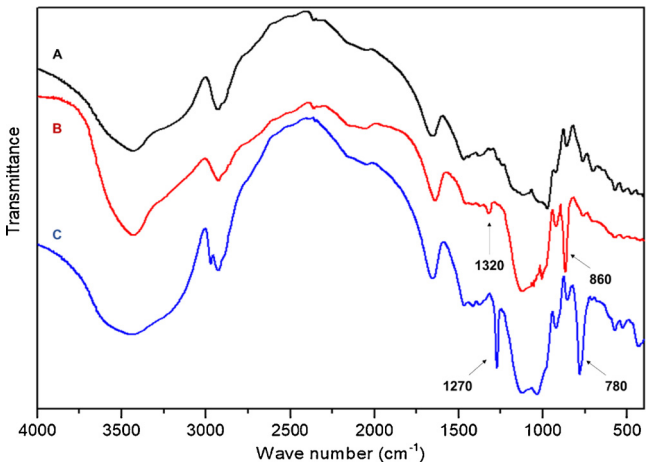

Fig. 1. Infrared spectrum of the starches: (A) without modification, (B) modified with CPMS, (C) modified with MTMS.

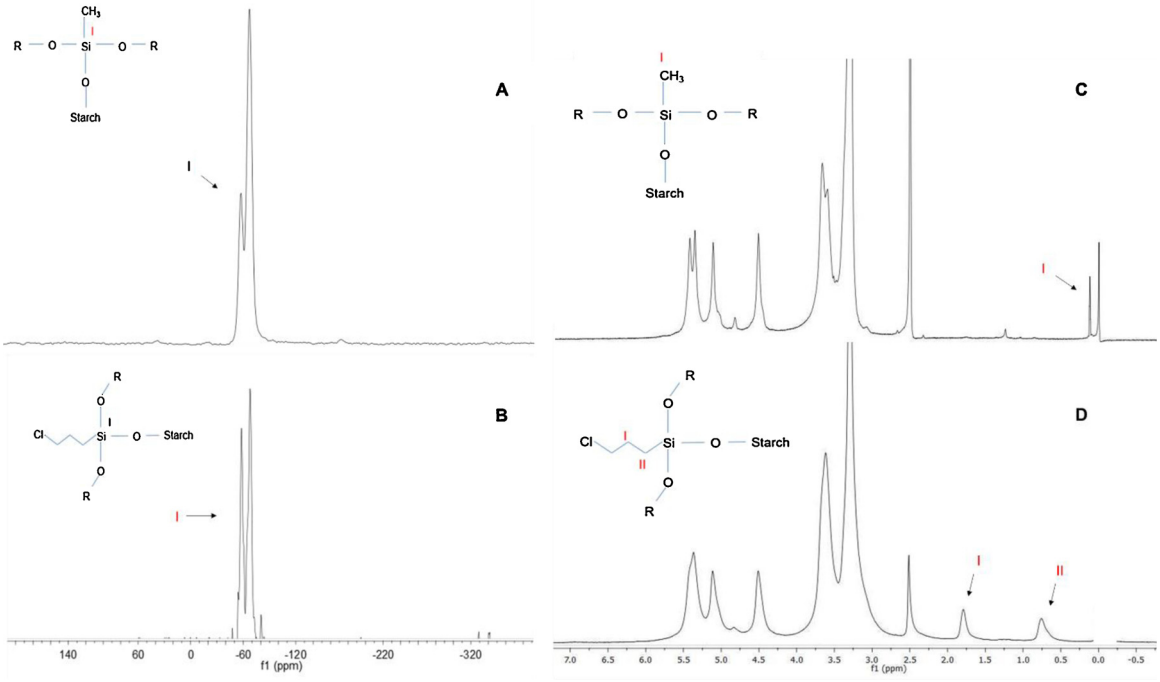

Fig. 2. ^{29}Si NMR spectra of (A) MTMS starch and (B) CPMS starch and ^{1}H NMR spectra of (C) MTMS starch and (D) CPMS starch.

the vibrations of CH_2-Cl bonds, respectively (Jariyasakoolroj & Chirachanchai, 2014). In Fig. 1C two intense peaks can be seen at 1270 cm^{-1} and 780 cm^{-1}. These peaks correspond to the vibrations of O-Si − CH_3 bonds, and are characteristic of MTMS (Zollfrank, 2001).

The ^{29}Si NMR spectra allow the identification of the different forms of silicon atoms bonds in the analyzed samples. Fig. 2 shows the ^{29}Si-NMR spectra of TPS-MTMS (A) and TPS-CPMS (B). Two main peaks can easily be identified at -58 ppm and-65 ppm in both spectra. According to Pickering, Abdalla, Ji, McDonald, and Franich, (2003), peaks at -58 ppm are indicative of Si-O groups bonded to saturated carbon such as carbohydrate (starch, cellulose, etc.). Zhang, Tingaut, Rentsch, Zimmermann, and Sèbe, (2015) explains that a strong signal near -56 ppm is consistent with the occurrence of chemical bonds between MTMS and cellulose. Therefore, the presence of the peak at -58 ppm can confirm the bonds between the Si groups and the starch chains. The peak at -65 ppm corresponds to silicon atoms attached to three Si-O groups (siloxane bridges) (Robles, Csóka, & Labidi, 2018; Zhang et al., 2015). These bonds tend to form structures called silsesquioxanes (Loy, Baugher, Baugher, Schneider, & Rahimian, 2000). Silsesquioxanes may be related to crosslinking of silylated starches (Jariyasakoolroj & Chirachanchai, 2014).

^{1}H-NMR spectra were analyzed to identify possible structures of the modified starches. Although silane-modified starches were carefully dissolved in D-DMSO, they did not show complete solubility. Fig. 2CD shows the spectra of TPS-MTMS (C) and TPS-CPMS (D). It can be noted that in both spectra there are the same peaks between 5.5 ppm and 2.5 ppm. Peaks between 5.5 ppm and 3 ppm correspond to starch backbone and peak at 2.5 ppm corresponds to DMSO (Baishya & Maji, 2014; Bunkerd et al., 2018; Elomaa et al., 2004). In the spectrum of Fig. 2a, the peak at 0.15 ppm (I) indicates the presence of Si − CH_3 (I) present in the MTMS structure (El Rassy & Pierre, 2005). The presence of this peak shows that the reaction between starch and silane occurred from the MTMS Si-O groups (the possible structure is shown in Fig.2C). The spectrum of Fig. 2b shows peaks at 1.75 ppm and 0.74 ppm. These peaks are characteristic of the CPMS and correspond to the protons of the groups − CH2- (I) and − CH2- (II) respectively, with the first group being closer to other carbons and the second group being closer to the Si atom (Jariyasakoolroj & Chirachanchai, 2014). Analyzing the Si and H spectra presented, it can be seen that the reaction between CPMS and starch occurred similarly to that of MTMS with starch (the possible modified starch structure is shown in Fig. 2D).

The degree of substitution (DS) analysis of the modified starches was performed following the methods used by Klemm et al. (2004); Petzold et al. (2003) and Staroszczyk and Janas (2010). The TPS-CPMS showed DS of 0.5 while TPS-MTMS showed DS of 1.1. One explanation for these values is that silylation using CPMS adds more spacious groups to the starch chain. Silylation with MTMS adds less spacious groups and consequently they stabilize more in the starch chain. MTMS also hydrolyzes more easily in water compared to CPMS, which helps in carrying out the reaction.

3.2. Density of the foams

Table 2 presents the density of the analyzed samples. TPS foam without any silylated starch in its composition showed the lowest density (142.8 kg/m^3) while the foams with higher silane concentrations presented higher densities. TPS-CPMS.40 and TPS-MTMS.40 foams presented the highest densities among the analyzed foams (220.3 and 226.6 kg/m^3, respectively). These values are higher than those found for EPS (60 kg/m^3), but lower than those found in other recent studies involving TPS foams (Mello & Mali, 2014; Pornsuksomboon, Holló, Szécsényi, & Kaewtatip, 2016; Uslu & Polat, 2012). The silanes

Table 2
Density, cell area and cell density of the analyzed foams.

Samples	Density (kg/m^3)	Average cell area (mm^2)	Cell density (cell/cm^3)
TPS	142.8 ± 5.1	0.2687	4.19×10^8
TPS-CPMS.10	151.4 ± 12.1	0.2545	4.75×10^8
TPS-CPMS.20	179.6 ± 5.5	0.2459	5.14×10^8
TPS-CPMS.30	184.4 ± 12.7	0.2302	4.38×10^8
TPS-CPMS.40	220.3 ± 3.9	0.2179	4.97×10^8
TPS-MTMS.10	150.8 ± 10.5	0.2539	4.77×10^8
TPS-MTMS.20	160.3 ± 11.7	0.2351	4.69×10^8
TPS-MTMS.30	191.9 ± 8.6	0.2226	4.91×10^8
TPS-MTMS.40	226.6 ± 12.4	0.2063	5.02×10^8

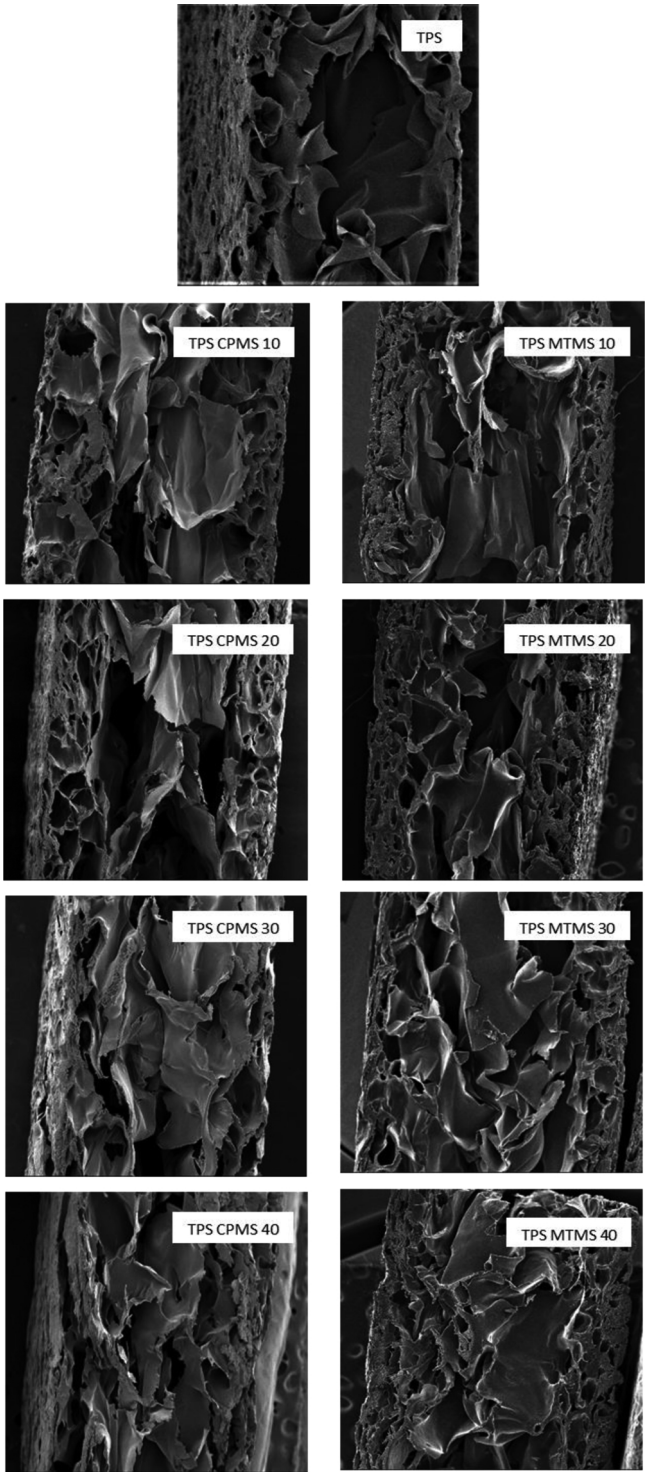

Fig. 3. SEM micrographs of cross-sectional surface of TPS foam, TPS CPMS and TPS MTMS foams.

present in the modified starch tend to form a crosslinking network between the starch chains (Jariyasakoolroj & Chirachanchai, 2014). Consequently, these crosslinks increase the viscosity of starch pastes. Due to this increase in viscosity the foam density became higher (Petzold et al., 2003; Staroszczyk & Janas, 2010; Staroszczyk, 2009).

3.3. Morphology of the foams

The SEM micrographs of the TPS, TPS-CPMS and TPS-MTMS cross sections are shown in Fig. 3. Starch foams made by the mold compression process or baking process form foams with the characteristic structure of this method, called the sandwich structure (Bergel, da Luz et al., 2018). This structure is characterized by having denser outer layers with small cells and having an inner layer with larger and more expanded cells. The water vapor that is released during the process acts as an blowing agent and forms the foam cells. During the process, the vapor bubbles tend to be larger in the center, forming larger cells, and smaller in the extremities, where it form smaller cells (Shogren, Lawton, Doane et al., 1998; Shogren, Lawton, Tiefenbacher, & Chen, 1998; Bergel et al., 2017; Bergel, da Luz et al., 2018; Cinelli, Chiellini, Lawton, & Imam, 2006; Matsuda, Verceheze, Carvalho, Yamashita, & Mali, 2013; Vercelheze et al., 2012).

Some changes can be seen with the addition of silylated starches in the foams. Compared to TPS foam, the silylated starch foams had a more compact structure and thicker outer layers. It can be noted that foams with lower amounts of silylated starch (TPS-CPMS 10 and 20 and TPS-MTMS 10 and 20) show better defined outer and inner layers, while foams with higher amounts of modified starch (TPS-CPMS.40 and TPS-MTMS.40) basically presented a unique structure that joins external and internal layer characteristics. The more compact structure of these foams, as well as the increased density with increasing amount of silane, can be explained by the higher viscosity of the silylated starch pastes that originated these foams (Mormann & Wagner, 1997). Due to the increase in paste viscosity caused by silane crosslinking, the rate of vapor bubbles expansion decreases. Consequently, it is more difficult for water vapor to expand the starch paste during the process. As a result, the foams become more compact and dense (Kaewtatip, Poungroi, Holló, & Mészáros Szécsényi, 2014; Lawton, Shogren, & Tiefenbacher, 1999; Soykeabkaew, Supaphol, & Rujiravanit, 2004, 2015). Pornsuksomboon et al. (2016) produced citric acid modified starch foams and reported that the crosslinking of the starch caused by the modification decreased chain mobility and consequently decreased paste expansion and increased the foam density. In the previous work, with starch foams containing acetylated starch and esterified starch, increasing the modified starch content decreased the viscosity of the pastes. As a result, the foams with more modified starch expanded more and became more porous, which affected their properties (Bergel, da Luz et al., 2018).

As shown in Table 2, average cell area and cell density tend to decrease and increase, respectively, as the amount of silylated starch increases in the samples. While the average cell area and cell density values of the TPS foam were 0.2687 mm^2 and 4.19 $\times$ 10^8 $cell/cm^3$ respectively, the values for the TPS-MTMS.40 foam were 0.2063 mm^2 and 5.02 $\times$ 10^8 $cell/cm^3$ respectively. During the foaming process, when there is a large expansion of the paste, the cells become so large that they absorb the smaller cells around them. Thus, these foams tend to have a larger cell area and lower cell density (due to fusion between cells) (Rizvi, Park, & Guo, 2008). Due to the reduced expansion of TPS foams with silylated starch, there is a less tendency for cells to join to form larger cells. Consequently, while cell area decreases (small cells) cell number and cell density increase.

3.4. Contact angle of TPS foams

Contact angle is an important test for analyzing the surface polarity of TPS foams. Angles were measured after 3 s of surface water drop deposition (initial contact angle) and then 3 min after deposition to study drop spreading and surface wettability. Table 3 presents the contact angles measured on the surface of the TPS foams analyzed in this paper. The results show that in general the modified starch foams presented a larger contact angle than the unmodified foams, indicating that there is less wettability of the drops on these surfaces. Consequently, these surfaces are more hydrophobic than the surfaces of unmodified foams (Jariyasakoolroj & Chirachanchai, 2014; Rhim, Lee, & Ng, 2007). After 3 min, new values were measured and it is noted that

Table 3
Contact angle (initial and after 3 min) of the analyzed TPS foams.

Sample	Contact Angle (after 3 s)	Contact Angle (after 3 min)
TPS	72.2 ± 2.7	67.5 ± 2.5
TPS-CPMS 10	75.4 ± 3.7	68.7 ± 3.5
TPS-CPMS 20	82.2 ± 4.2	73.7 ± 3.7
TPS-CPMS 30	80.0 ± 3.3	75.4 ± 2.7
TPS-CPMS 40	81.4 ± 4.2	74.2 ± 2.9
TPS-MTMS 10	84.4 ± 1.3	76.6 ± 3.0
TPS-MTMS 20	81.5 ± 3.5	73.9 ± 3.2
TPS-MTMS 30	85.6 ± 3.0	75.1 ± 2.6
TPS-MTMS 40	87.5 ± 2.5	76.3 ± 3.2

all angles were smaller than the initial ones, indicating the beginning of the absorption of the water drop on the surface. Even so, after this period, the drop angles on the surfaces of the modified foams are larger than the angles on the surfaces of the unmodified foams. Xiong et al. (2014) also modified starch with more hydrophobic molecules and also noted the increased contact angle on the surface of modified starches compared to natural starch. Fig. 4 shows the images of the drops deposited on TPS, TPS-CPMS.20 and TPS-MTMS.40 foams within 3 s (the foams with the highest contact angle within their respective groups). It can be seen that there is a larger spread of water drop on the TPS foam surface compared to the drops on the TPS-CPMS and TPS-MTSM foam surfaces.

The irregular variation in contact angles may be due to the irregular surface that starch foams usually have. As the foam structure is produced by the violent release of steam, the outer (thicker) layers are not completely smooth after the foam comes out of the form. Due to these surface irregularities, water droplets can accommodate this surface in different ways. Because of this, foams that are supposed to have greater hydrophobicity may not show a significant increase in the average of contact angles and may even have slightly lower contact angles.

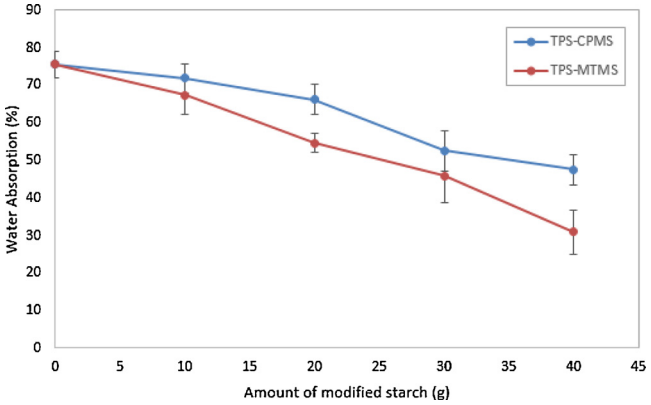

Fig. 5. Water absorption of the TPS foams in 5 min.

3.5. Water absorption of TPS foams

Water absorption behavior has a great influence on the shelf life of packaging, as it influences the dimensional stability and mechanical properties of materials. Fig. 5 shows the water absorption results of TPS foams. Foam contact time with water was 5 min. TPS-CPMS and TPS-MTMS foams showed a tendency to decrease water absorption with increasing amount of silanized starch used. TPS foam absorbed 75 g water/100 g solids, while TPS-CPMS.10, TPS-CPMS.20, TPS-CPMS.30 and TPS-CPMS.40 foams absorbed 72, 66, 52 and 47 g water/100 g solids respectively. TPS-MTMS.10, TPS-MTMS.20, TPS-MTMS.30 and TPS-MTMS.40 foams absorbed 67, 54, 46 and 31 g water/100 g solids respectively. It can be noted that the higher the silane content, the lower the water absorption, which indicates that the hydrophobization was effective. TPS-CPMS.40 and TPS-MTMS.40 foams absorbed approximately 28 % and 45 % less water than unmodified foam, respectively. This indicates that silane groups replaced some hydroxyl groups

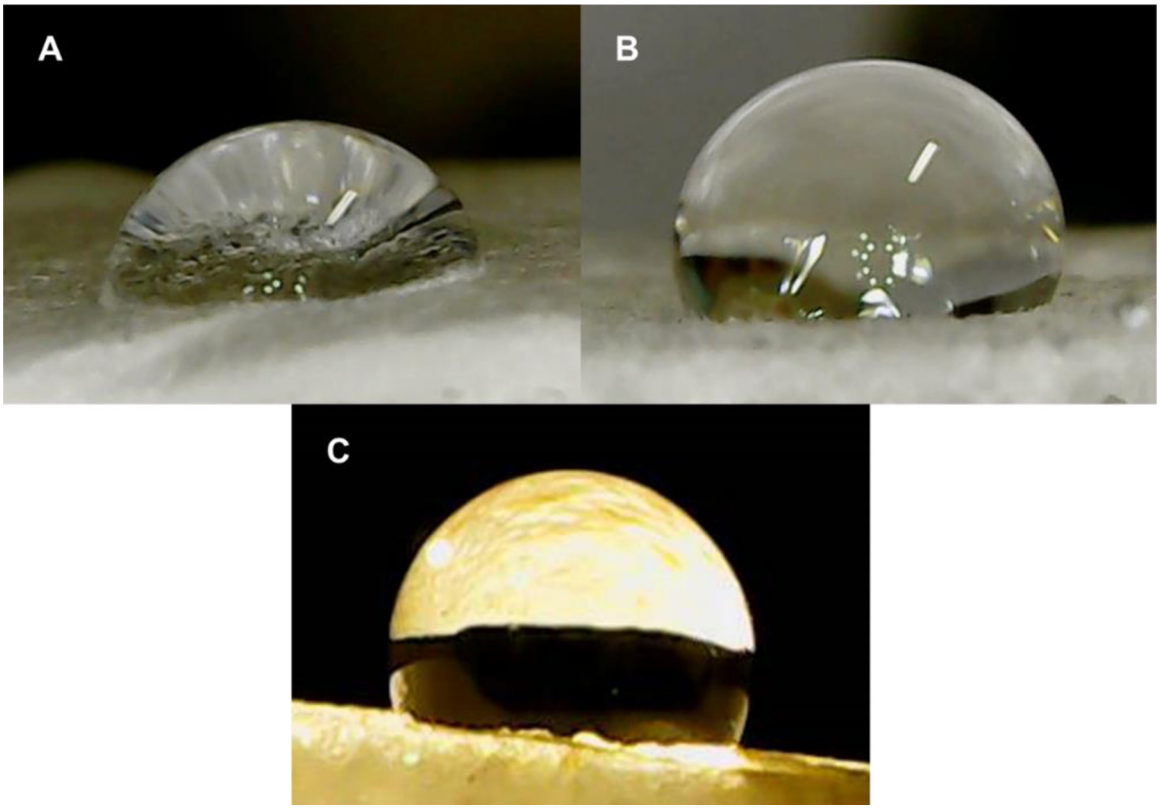

Fig. 4. Water contact angle of foams: TPS (A), TPS CPMS.20 (B) and TPS MTMS.40 (C).

in the starch structure, which made the material more resistant to water contact (Wei et al., 2016). Wei et al. (2016) researched the synthesis of a silane in starch nanocrystals and showed that the higher the silane content in starch, the lower its affinity for water. The apparent lower water absorption of TPS-MTMS foams compared to TPS-CPMS foams, seen mainly when comparing TPS-MTMS.40 and TPS-CPMS.40 foams, may be due to the higher degree of substitution of silylated starch with MTMS (1.1 DS) over to silylated starch with CPMS (0.5 DS). Other authors have also reported increased starch hydrophobicity when it is silylated (Jariyasakoolroj & Chirachanchai, 2014; Moad, 2011; Staroszczyk & Janas, 2010; Staroszczyk, Tomasik, Janas, & Poreda, 2007; Staroszczyk, 2009). In the previous study, acetylation and esterification were tested to hydrophobize the starch used in the foams (Bergel, da Luz et al., 2018). Comparing the efficiency of hydrophobization in water absorption, TPS-CPMS.40 foam showed similar water absorption results to foams with 13.34 % w/w acetylated starch (TPS Ac.20) and 20 % w/w of esterified starch (TPS Es.30), that were the foams that absorbed less water in the previous study, 42 and 45 g water/g solids. TPS-MTMS.40 foam was the foam that absorbed less water among the foams analyzed in these studies, indicating that this type of silylation is more efficient than the other techniques presented (Bergel, da Luz et al., 2018).

3.6. Moisture absorption of TPS foams

Starch-based foams tend to exhibit changes in their physical and mechanical properties when in low or high humidity environments. When these materials are in high humidity environments their mechanical resistance decreases. According to Soykeabkaew et al. (2015) the mechanical properties of this type of foam reach their maximum with a moisture content of 0.075 g water/g solids, above this value the mechanical resistance decreases. Moisture absorption over time of the TPS-CPMS foams at 90 % RH (ambient relative humidity) is shown in Fig. 6A. The equilibrium moisture content of the TPS foam at 120 h (final measurement) was 0.2317 g water / g solids, while for TPS-CPMS.10, TPS-CPMS.20, TPS-CPMS.30 and TPS-CPMS.40 foams was 0.2215, 0.1843, 0.1685 and 0.1621 g water/g solid, respectively. As the presence of hydrophobic silane groups increased in the foams, the greater the moisture resistance became (Staroszczyk & Janas, 2010; Staroszczyk, 2009). The higher density and smaller porosity (smaller cells) of the silylated starch foams may also have influenced the lower moisture absorption of these foams.

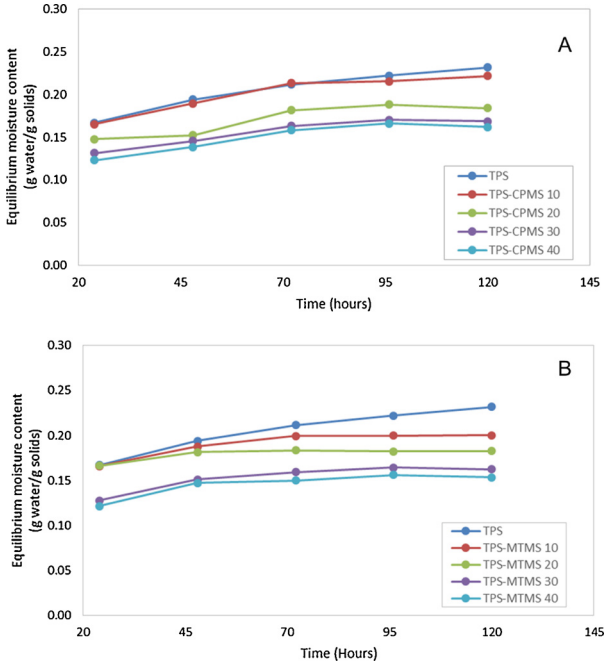

Fig. 6. Moisture absorption of TPS foam: (A) TPS CPMS and (B) TPS MTMS foams at 90 % RH.

Fig. 6B shows the moisture absorption of MTMS foams. It can be seen that TPS-MTMS foams also had higher moisture resistance compared to unmodified TPS foams. In 120 h, TPS-MTMS.10, TPS-MTMS.20, TPS-MTMS.30 and TPS-MTMS.40 foams absorbed 0.2001, 0.1826, 0.1623 and 0.1531 respectively. These results show that MTMS modification considerably increased the moisture resistance of the foams. Zhang et al. (2015) used MTMS to silanize cellulose fibers and the results also showed that MTMS highly hydrophobized cellulose.

To investigate moisture sorption kinetics, the data obtained were analyzed using the Peleg (1988) mathematical model, a mathematical model developed to analyze the moisture absorption kinetics of foods (Paquet-Durand, Zettel, & Hitzmann, 2015; Sopade, Xun, Halley, & Hardin, 2007). Peleg K1 and K2 constants for TPS, TPS CPMS and TPS MTMS foams are shown in Table 4. K1 represents mass transfer. The lower the K1, the higher the initial foam absorption rate. K2 represents the maximum absorption capacity. Similarly, the lower the K2, the greater the absorption capacity of the foam.

TPS-CPMS and TPS-MTMS foams presented higher K1 and K2 than TPS foam, indicating that these foams have a lower capacity to absorb water. However, the TPS-CPMS.10 foam showed almost the same K2 as unmodified TPS, indicating a similar maximum absorption capacity. These foams presented very similar values of water and moisture absorption, which justifies their constants having close values. The K1 constants of the TPS-CPMS and TPS-MTMS foams increased as silane content increased. This can be explained by the increased density and decreased porosity of these foams, as the initial absorption of the foam is more closely related to porosity (Mello & Mali, 2014; Vercelheze et al., 2012). The constant K2 also increased with increasing amount of silanes. While the K2 value was 5.89 for the unmodified foam, the value was 7.59 and 9.30 for the TPS-CPMS.40 and TPS-MTMS.40 foams respectively. This indicates a lower maximum absorption capacity and greater hydrophobicity (Mello & Mali, 2014; Staroszczyk & Janas, 2010).

3.7. Mechanical properties of TPS foams

Table 4 presents the results of the flexural test of the analyzed TPS foams. Starch foams often exhibit anisotropic structure and brittleness, as the rigidity of the foam surface is significantly greater than that of the center. When the foam is flexed, the surface is subjected to the highest stress values. The presented results show that the flexural modulus and the flexural strength increased with the addition of silylated starch in the foams and it can be noted that the higher the proportion of silylated starch present, the greater the modulus and flexural strength. The TPS presented modulus of 127.62 MPa and flexural strength of 0.51 MPa while the TPS-CPMS and TPS-MTMS foams presented modulus of 253.45 MPa and 235.26 MPa and flexural strength of 3.21 MPa and 3.32 MPa. The elongation at break showed no significant changes. Table 5 also presents the impact resistance results. While the TPS-CPMS.10 (13.52 J/m) foam showed impact resistance close to that found for normal TPS (12.33 J/m), the other TPS-CPMS and TPS-MTMS foams presented higher impact resistance. TPS-CPMS.40 and TPS-MTMS presented the highest density (0.2203 and 0.2266 g/cm^3) and the highest impact strength (18.71 and 17.27 J/m). The increase in these mechanical properties may be due to the structure of these foams. Crosslinking caused by silanes made the starch pastes more viscous and consequently formed denser foams with a thicker and more rigid outer layer (Shogren, Lawton, Tiefenbacher et al., 1998; Jariyasakoolroj & Chirachanchai, 2014; Zhang et al., 2015). Shogren, Lawton, Tiefenbacher et al. (1998) explain that crosslinking probably increases the effective molecular weight of starch, thereby increasing the force necessary to cause crack and fracture formation. Pornsuksomboon,

Table 4
Mechanical properties of the analyzed foams and the Peleg constants.

Samples	Flexural modulus (MPa)	Flexural strength (MPa)	Elongation at break (%)	Impact strength (J/m)	Peleg Constants	
					K1	K2
TPS	127.62 ± 15.22	0.51 ± 0.10	1.68 ± 0.26	12.33 ± 0.52	86.69	5.89
TPS CPMS 10	122.45 ± 10.39	1.16 ± 0.21	1.24 ± 0.17	13.52 ± 0.82	113.66	5.88
TPS CPMS 20	154.28 ± 21.81	2.20 ± 0.26	1.39 ± 0.33	16.75 ± 1.15	162.96	7.14
TPS CPMS 30	199.19 ± 15.69	2.33 ± 0.38	1.53 ± 0.37	16.58 ± 0.55	137.10	7.73
TPS CPMS 40	253.45 ± 32.11	321 ± 0.48	1.22 ± 0.31	18.71 ± 0.49	181.74	7.59
TPS MTMS 10	140.66 ± 20.15	1.86 ± 0.61	1.65 ± 0.44	15.06 ± 0.97	142.50	7.23
TPS MTMS 20	147.30 ± 16.73	2.01 ± 0.25	1.77 ± 0.23	15.88 ± 1.28	116.70	8.20
TPS MTMS 30	182.35 ± 19.43	2.73 ± 0.40	1.59 ± 0.43	15.76 ± 1.60	170.01	8.72
TPS MTMS 40	235.26 ± 27.77	3.32 ± 0.34	2.02 ± 0.52	17.27 ± 1.01	165.70	9.30

Szécsényi, Holló, and Kaewtatip (2014) explain that the viscosity of the starch pastes forming the foams significantly influences the final morphology of the product. While low viscosities cause larger cells and thinner outer layer, high viscosities cause smaller cells and thicker outer layer. The authors also explain that large cells tend to reduce impact resistance. Kaewtatip et al. (2014) state that in modified starch foams, interactions between substituents may promote the formation of intermolecular bridges (cross-links) between polysaccharide chains, which may increase the impact resistance of these foams.

4. Conclusions

The addition of hydrophobized starches changed the structure and properties of TPS foams. Starch foams with silanized starch addition showed lower water absorption, lower moisture absorption, higher density and higher impact resistance. Except for increased density, all property changes are desirable in packaging. Between the two silanes analyzed, the foams with MTMS presented higher surface hydrophobicity and lower water absorption. Reaction with MTMS resulted in a higher substitution starch (1.1 DS) compared to CPMS (0.5 DS). This difference caused by the larger volume of the CPMS molecule makes MTMS a better choice for hydrophobizing starch. The MTMS 40 foam presented the most satisfactory results, as it presented stable structure, good impact resistance, high flexural strength and was the foam that absorbed less water.

Authors' contributions

B.F.B wrote the article, conducted and supervised the scientific tests.

L.L.A assisted and performed all scientific tests.

A.L.S.S supervised and assisted in obtaining the scanning electron microscopy images.

R.M.C.S supervised all research and assisted in theoretical research-related knowledge.

Acknowledgments

This work was supported by the National Council of Scientific and Technological Development of Brazil (CNPQ) and authors greatly thank the assistance. The authors also thank the laboratory of Polymeric Materials (LAPOL), the post graduated program of Materials Engineering (PPGEM), the SENAI Institute for innovation in Polymer Engineering, the Federal University of Rio Grande do Sul (UFRGS) and especially to the UFRGS Chemistry Institute.

References

Baishya, P., & Maji, T. K. (2014). Studies on effects of different cross-linkers on the properties of starch-based wood composites. *ACS Sustainable Chemistry and Engineering, 2*(7), 1760–1768. https://doi.org/10.1021/sc5002325.

Bénézet, J. C., Stanojlovic-Davidovic, A., Bergeret, A., Ferry, L., & Crespy, A. (2012). Mechanical and physical properties of expanded starch, reinforced by natural fibres. *Industrial Crops and Products, 37*(1), 435–440. https://doi.org/10.1016/j.indcrop.2011.07.001.

Bergel, B. F., da Luz, L. M., & Santana, R. M. C. (2017). Comparative study of the influence of chitosan as coating of thermoplastic starch foam from potato, cassava and corn starch. *Progress in Organic Coatings, 106*, 27–32. https://doi.org/10.1016/j.porgcoat.2017.02.010.

Bergel, B. F., da Luz, L. M., & Santana, R. M. C. (2018). Effect of poly(lactic acid) coating on mechanical and physical properties of thermoplastic starch foams from potato starch. *Progress in Organic Coatings, 118*, 91–96. https://doi.org/10.1016/j.porgcoat.2018.01.029.

Bergel, B. F., Dias Osorio, S., da Luz, L. M., & Santana, R. M. C. (2018). Effects of hydrophobized starches on thermoplastic starch foams made from potato starch. *Carbohydrate Polymers, 200*, 106–114. https://doi.org/10.1016/j.carbpol.2018.07.047.

Blackwell, J. M., Foster, K. L., Beck, V. H., & Piers, W. E. (1999). B(C6F5)3-catalyzed silation of alcohols: A mild, general method for synthesis of silyl ethers. *Journal of Organic Chemistry, 64*(13), 4887–4892. https://doi.org/10.1021/jo9903003.

Bunkerd, R., Molloy, R., Somsunan, R., Punyodom, W., Topham, P. D., & Tighe, B. J. (2018). Synthesis and characterization of chemically-modified cassava starch grafted with poly(2-ethylhexyl acrylate) for blending with poly(Lactic acid). *Starch/Staerke, 70*(11–12), 1–10. https://doi.org/10.1002/star.201800093.

Carr, L. G., Parra, D. F., Ponce, P., Lugão, A. B., & Buchler, P. M. (2006). Influence of fibers on the mechanical properties of cassava starch foams. *Journal of Polymers and the Environment, 14*, 179–183. https://doi.org/10.1007/s10924-006-0008-5.

Cinelli, P., Chiellini, E., Lawton, J. W., & Imam, S. H. (2006). Foamed articles based on potato starch, corn fibers and poly(vinyl alcohol). *Polymer Degradation and Stability, 91*(5), 1147–1155. https://doi.org/10.1016/j.polymdegradstab.2005.07.001.

Clemente, C. C. C., Paresque, K., & Santos, P. J. P. (2018). The effects of plastic bags presence on a macrobenthic community in a polluted estuary. *Marine Pollution Bulletin, 135*(July), 630–635. https://doi.org/10.1016/j.marpolbul.2018.07.070.

Compa, M., Alomar, C., Wilcox, C., van Sebille, E., Lebreton, L., Hardesty, B. D., et al. (2019). Risk assessment of plastic pollution on marine diversity in the Mediterranean Sea. *Science of the Total Environment, 678*, 188–196. https://doi.org/10.1016/j.scitotenv.2019.04.355.

Dikareva, N., & Simon, K. S. (2019). Microplastic pollution in streams spanning an urbanisation gradient. *Environmental Pollution, 250*, 292–299. https://doi.org/10.1016/j.envpol.2019.03.105.

El Rassy, H., & Pierre, A. C. (2005). NMR and IR spectroscopy of silica aerogels with different hydrophobic characteristics. *Journal of Non-Crystalline Solids, 351*(19–20), 1603–1610. https://doi.org/10.1016/j.jnoncrysol.2005.03.048.

Elomaa, M., Asplund, T., Soininen, P., Laatikainen, R., Peltonen, S., Hyvärinen, S., et al. (2004). Determination of the degree of substitution of acetylated starch by hydrolysis, 1 H NMR and TGA/IR. *Carbohydrate Polymers, 57*, 261–267. https://doi.org/10.1016/j.carbpol.2004.05.003.

Glenn, G. M., Orts, W. J., & Nobes, G. A. R. (2001). Starch, fiber and CaCo3 effects on the physical properties of foams made by a baking process. *Industrial Crops and Products, 14*(3), 201–212. https://doi.org/10.1016/S0926-6690(01)00085-1.

Jariyasakoolroj, P., & Chirachanchai, S. (2014). Silane modified starch for compatible reactive blend with poly (lactic acid). *Carbohydrate Polymers, 106*, 255–263. https://doi.org/10.1016/j.carbpol.2014.02.018.

Jepsen, E. M., & de Bruyn, P. J. N. (2019). Pinniped entanglement in oceanic plastic pollution: A global review. *Marine Pollution Bulletin, 145*(December), 295–305. https://doi.org/10.1016/j.marpolbul.2019.05.042.

Kaewtatip, K., Poungroi, M., Holló, B., & Mészáros Szécsényi, K. (2014). Effects of starch types on the properties of baked starch foams. *Journal of Thermal Analysis and Calorimetry, 115*(1), 833–840. https://doi.org/10.1007/s10973-013-3149-5.

Klemm, D., Philipp, B., Heinze, T., Heinze, U., & Wagenknecht, W. (2004). *Comprehensive Cellulose Chemistry: Fundamentals and Analytical Methods*.

Lawton, J. W., Shogren, R. L., & Tiefenbacher, K. F. (1999). Effect of batter solids and starch type on the structure of baked starch foams. *Cereal Chemistry, 76*(5), 682–687. https://doi.org/10.1094/CCHEM.1999.76.5.682.

Lima, B. N. B., Cabral, T. B., Roberto, P., Neto, C., Tavares, M. I. B., & Pierucci, A. P. T. (2012). Estudo do Amido de Farinhas Comerciais Comestíveis. *Polímeros, 22*(5), 486–490. https://doi.org/10.1590/S0104-14282012005000062.

Loy, D. A., Baugher, B. M., Baugher, C. R., Schneider, D. A., & Rahimian, K. (2000). Substituent effects on the sol-gel chemistry of organotrialkoxysilanes. *Chemistry of Materials, 12*(12), 3624–3632. https://doi.org/10.1021/cm000451i.

Matsuda, D. K. M., Verceheze, A. E. S., Carvalho, G. M., Yamashita, F., & Mali, S. (2013). Baked foams of cassava starch and organically modified nanoclays. *Industrial Crops and Products, 44*, 705–711. https://doi.org/10.1016/j.indcrop.2012.08.032.

Mello, L. R. P. F., & Mali, S. (2014). Use of malt bagasse to produce biodegradable baked foams made from cassava starch. *Industrial Crops and Products, 55*, 187–193. https://doi.org/10.1016/j.indcrop.2014.02.015.

Menicagli, V., Balestri, E., Vallerini, F., Castelli, A., & Lardicci, C. (2019). Adverse effects of non-biodegradable and compostable plastic bags on the establishment of coastal dune vegetation: First experimental evidences. *Environmental Pollution, 252*, 188–195. https://doi.org/10.1016/j.envpol.2019.05.108.

Moad, G. (2011). Chemical modification of starch by reactive extrusion. *Progress in Polymer Science (Oxford), 36*(2), 218–237. https://doi.org/10.1016/j.progpolymsci.2010.11.002.

Mormann, W., & Wagner, T. (1997). Silylation of cellulose and low-molecular-weight carbohydrates with hexamethyldisilazane in liquid ammonia. *Macromolecular Rapid Communications, 18*(6), 515–522. https://doi.org/10.1002/marc.1997.030180610.

Paquet-Durand, O., Zettel, V., & Hitzmann, B. (2015). Optimal experimental design for parameter estimation of the Peleg model. *Chemometrics and Intelligent Laboratory Systems, 140*, 36–42. https://doi.org/10.1016/j.chemolab.2014.10.006.

Peleg, M. (1988). An empirical model for the description moisture sorption curves. *Journal of Food Science, 53*(4), 1216–1217.

Petzold, K., Koschella, A., Klemm, D., Heublein, B., & Jena, D.- (2003). Silylation of cellulose and starch—Selectivity, structure analysis and subsequent reactions. *Cellulose, 10*, 251–269.

Pickering, K. L., Abdalla, A., Ji, C., McDonald, A. G., & Franich, R. A. (2003). The effect of silane coupling agents on radiata pine fibre for use in thermoplastic matrix composites. *Composites Part A: Applied Science and Manufacturing, 34*(10), 915–926. https://doi.org/10.1016/S1359-835X(03)00234-3.

Pornsuksomboon, K., Holló, B. B., Szécsényi, K. M., & Kaewtatip, K. (2016). Properties of baked foams from citric acid modified cassava starch and native cassava starch blends. *Carbohydrate Polymers, 136*, 107–112. https://doi.org/10.1016/j.carbpol.2015.09.019.

Pornsuksomboon, K., Szécsényi, K. M., Holló, B., & Kaewtatip, K. (2014). Preparation of native cassava starch and cross-linked starch blended foams. *Standardization News, 66*(9–10), 818–823. https://doi.org/10.1002/star.201400031.

Qi, Q., Wu, Y., Tian, M., Liang, G., Zhang, L., & Ma, J. (2006). Modification of starch for high performance elastomer. *Polymer, 47*(11), 3896–3903. https://doi.org/10.1016/j.polymer.2006.03.095.

Qu, J., & He, L. (2013). Synthesis and properties of silane-fluoroacrylate grafted starch. *Carbohydrate Polymers, 98*(1), 1156–1164. https://doi.org/10.1016/j.carbpol.2013.07.015.

Rhim, J. W., Lee, J. H., & Ng, P. K. W. (2007). Mechanical and barrier properties of biodegradable soy protein isolate-based films coated with polylactic acid. *LWT - Food Science and Technology, 40*(2), 232–238. https://doi.org/10.1016/j.lwt.2005.10.002.

Rizvi, G. M., Park, C. B., & Guo, G. (2008). Strategies for processing wood plastic composites with chemical blowing agents. *Journal of Cellular Plastics, 44*(2), 125–137. https://doi.org/10.1177/0021955X07082184.

Robles, E., Csóka, L., & Labidi, J. (2018). Effect of reaction conditions on the surface modification of cellulose nanofibrils with aminopropyl triethoxysilane. *Coatings, 8*(4), https://doi.org/10.3390/coatings8040139.

Shogren, R. L., Lawton, J. W., Doane, W. M., & Tiefenbacher, K. F. (1998). Structure and morphology of baked starch foams. *Polymer, 39*(25), 6649–6655. https://doi.org/10.1016/S0032-3861(97)10303-2.

Shogren, R. L., Lawton, J. W., Tiefenbacher, K. F., & Chen, L. (1998). Starch-poly(vinyl alcohol) foamed articles prepared by a baking process. *Journal of Applied Polymer Science, 68*(13), 2129–2140. https://doi.org/10.1002/(SICI)1097-4628(19980627)68:13<2129::AID-APP9>3.0.CO;2-E.

Sopade, P. A., Xun, P. Y., Halley, P. J., & Hardin, M. (2007). Equivalence of the Peleg, Pilosof and Singh-Kulshrestha models for water absorption in food. *Journal of Food Engineering, 78*(2), 730–734. https://doi.org/10.1016/j.jfoodeng.2005.10.007.

Soykeabkaew, N., Supaphol, P., & Rujiravanit, R. (2004). Preparation and characterization of jute- and flax-reinforced starch-based composite foams. *Carbohydrate Polymers, 58*(1), 53–63. https://doi.org/10.1016/j.carbpol.2004.06.037.

Soykeabkaew, N., Thanomsilp, C., & Suwantong, O. (2015). A review: Starch-based composite foams. *Composites Part A: Applied Science and Manufacturing, 78*, 246–263. https://doi.org/10.1016/j.compositesa.2015.08.014.

Staroszczyk, H. (2009). Microwave-assisted silication of potato starch. *Carbohydrate Polymers, 77*(3), 506–515. https://doi.org/10.1016/j.carbpol.2009.01.025.

Staroszczyk, H., & Janas, P. (2010). Microwave-assisted preparation of potato starch silicated with silicic acid. *Carbohydrate Polymers, 81*(3), 599–606. https://doi.org/10.1016/j.carbpol.2010.03.017.

Staroszczyk, H., Tomasik, P., Janas, P., & Poreda, A. (2007). Esterification of starch with sodium selenite and selenate. *Carbohydrate Polymers, 69*(2), 299–304. https://doi.org/10.1016/j.carbpol.2006.10.009.

Uslu, M. K., & Polat, S. (2012). Effects of glyoxal cross-linking on baked starch foam. *Carbohydrate Polymers, 87*(3), 1994–1999. https://doi.org/10.1016/j.carbpol.2011.10.008.

Vercelheze, A. E. S., Fakhouri, F. M., Dall, L. H., Urbano, A., Youssef, E. Y., & Yamashita, F. (2012). Properties of baked foams based on cassava starch, sugarcane bagasse fibers and montmorillonite. *Carbohydrate Polymers, 87*(2), 1302–1310. https://doi.org/10.1016/j.carbpol.2011.09.016.

Volkert, B., Lehmann, A., Greco, T., & Nejad, M. H. (2010). A comparison of different synthesis routes for starch acetates and the resulting mechanical properties. *Carbohydrate Polymers, 79*(3), 571–577. https://doi.org/10.1016/j.carbpol.2009.09.005.

Wang, W., Guan, L., Seib, P. A., & Shi, Y. (2018). Settling volume and morphology changes in cross-linked and unmodified starches from wheat, waxy wheat, and waxy maize in relation to their pasting properties. *Carbohydrate Polymers, 196*(April), 18–26. https://doi.org/10.1016/j.carbpol.2018.05.009.

Wei, B., Sun, B., Zhang, B., Long, J., Chen, L., & Tian, Y. (2016). Synthesis, characterization and hydrophobicity of silylated starch nanocrystal. *Carbohydrate Polymers, 136*, 1203–1208. https://doi.org/10.1016/j.carbpol.2015.10.025.

Wokadala, O. C., Emmambux, N. M., & Ray, S. S. (2014). Inducing PLA/starch compatibility through butyl-etherification of waxy and high amylose starch. *Carbohydrate Polymers, 112*, 216–224. https://doi.org/10.1016/j.carbpol.2014.05.095.

Wu, Y. P., Qi, Q., Liang, G. H., & Zhang, L. Q. (2006). A strategy to prepare high performance starch/rubber composites: In situ modification during latex compounding process. *Carbohydrate Polymers, 65*(1), 109–113. https://doi.org/10.1016/j.carbpol.2005.12.031.

Xiong, Z., Ma, S., Fan, L., Tang, Z., Zhang, R., Na, H., et al. (2014). Surface hydrophobic modification of starch with bio-based epoxy resins to fabricate high-performance polylactide composite materials. *Composites Science and Technology, 94*, 16–22. https://doi.org/10.1016/j.compscitech.2014.01.007.

Zhang, Z., Tingaut, P., Rentsch, D., Zimmermann, T., & Sèbe, G. (2015). Controlled silylation of nanofibrillated cellulose in water: Reinforcement of a model polydimethylsiloxane network. *ChemSusChem, 8*(16), 2681–2690. https://doi.org/10.1002/cssc.201500525.

Zollfrank, C. (2001). Silylation of solid beech wood. *Wood Science and Technology, 35*(1–2), 183–189. https://doi.org/10.1007/s002260000071.